

# Canonical Subproblems for Robot Inverse Kinematics

Alexander J. Elias and John T. Wen, *Fellow, IEEE*

**Abstract**—Inverse kinematics of many common types of robot manipulators may be decomposed into canonical subproblems. This paper presents new solution methods to six subproblems using a linear algebra approach. The first three subproblems, called the Paden–Kahan subproblems, are Subproblem 1: angle between a vector on the edge of a cone and a point, Subproblem 2: intersections between two cones, and Subproblem 3: intersections between a cone and a sphere. The other three subproblems, which have not been extensively covered in the literature, are Subproblem 4: intersections between a cone and a plane, Subproblem 5: intersections among three cones, and Subproblem 6: intersections in a system of four cones. We present algebraic solutions and geometric interpretations for each subproblem and provide computational performance comparisons. Our approach also finds the least-squares solutions for Subproblems 1–4 when the exact solution does not exist. We show that almost all 6-dof all revolute (6R) robots with known closed-form solutions may be solved using the subproblem decomposition method. For a general 6R robot, subproblem decomposition reduces finding all solutions to a search on a circle or a 2D torus. The software code is available on a publicly accessible repository.

**Index Terms**—Articulated Robot, Inverse Kinematics, Least-Squares Problem, Paden–Kahan Subproblem

## I. INTRODUCTION

**I**NVERSE KINEMATICS for 6-dof articulated all-revolute-joint (6R) robots has a long history. The seminal work by Pieper [1] reduced the inverse kinematics problem to solving the real roots of a 16th order polynomial. For certain cases of robots with intersecting or parallel axes, the solution may be simplified down to solving quartic, or even quadratic, polynomials. Paden later showed that for some of these special 6R robots, the inverse kinematics problem may be decomposed into a series of smaller canonical subproblems with closed-form solutions [2]. The influential robotics textbook [3] called these subproblems the Paden–Kahan Subproblems 1, 2, and 3.

The subproblem decomposition approach is an elegant and computationally efficient method, but it does not work for general 6R robots and does not provide least-squares solutions when numerical inaccuracies may prevent the exact solutions of these subproblems.

In this paper, we revisit the subproblem decomposition approach by introducing three new subproblems along with one subproblem extension. We state these subproblems both geometrically and algebraically, and present alternate closed-form solution methods as compared to those in [2] and subsequently used in [3] and other papers. Furthermore, for some of these subproblems, we also obtain the closed-form least-squares solutions when the exact solution does not exist.

The authors are with the Department of Electrical, Computer, and Systems Engineering, Rensselaer Polytechnic Institute, Troy, NY 12180 USA (e-mail: eliasa3@rpi.edu; wenj@rpi.edu).

TABLE I  
SUBPROBLEM FORMULATIONS

Subproblem	Equation
1: Cone and point	$\min_{\theta} \ R(k, \theta)p_1 - p_2\ $
2: Two cones	$\min_{\theta_1, \theta_2} \ R(k_1, \theta_1)p_1 - R(k_2, \theta_2)p_2\ $
2E: Two offset cones	$p_0 + R(k_1, \theta_1)p_1 = R(k_2, \theta_2)p_2$
3: Cone and sphere	$\min_{\theta} \ R(k, \theta)p_1 - p_2\  - d$
4: Cone and plane	$\min_{\theta}  h^T R(k, \theta)p - d $
5: Three cones	$p_0 + R(k_1, \theta_1)p_1 = R(k_2, \theta_2)(p_2 + R(k_3, \theta_3)p_3)$
6: Four cones	$\begin{cases} h_1^T R(k_1, \theta_1)p_1 + h_2^T R(k_2, \theta_2)p_2 = d_1 \\ h_3^T R(k_3, \theta_3)p_3 + h_4^T R(k_4, \theta_4)p_4 = d_2 \end{cases}$

The subproblems considered in this paper are summarized in Table I, where  $\theta$  is an unknown angle,  $p$  is an  $\mathbb{R}^3$  vector,  $h$  is a unit  $\mathbb{R}^3$  vector, and  $d$  is a scalar. ( $d$  must be positive in Subproblem 3.) We pose Subproblems 1, 2, 3, and 4 as least-squares problems, while Subproblems 2E, 5, and 6 are posed as exact equations. Note that  $R(k, \theta)$  denotes the rotation matrix about a unit vector  $k \in \mathbb{R}^3$  over an angle  $\theta$ . We call  $R(k, \theta)p$  for some fixed  $p$ ,  $k$  and parameter  $\theta$  a cone because as  $\theta$  varies, the tip of the rotated  $p$  sweeps out a circle while the tail stays in place, meaning each rotated vector  $p$  is on the curved face of a cone.

Numerous authors have contributed to the Paden–Kahan Subproblems, and several also proposed new subproblems. In [4]–[20], subproblems are solved using screw theory. In [16], subproblem solutions are provided with quaternions, and in [16], [21]–[23] dual quaternions are used. Several authors posed new subproblems with three consecutive rotations with constraints on which axes are parallel or intersecting, which are special cases of our Subproblem 5 [4], [6], [10], [11], [13], [15], [19], [22]. In [9], [20], the fully general case of three consecutive rotations is solved. In [5], [7], [8], [15], [19], a new subproblem of two consecutive rotations with an offset is posed, which is our Subproblem 2E. In [10], [13], [19], [23], the solution for two consecutive parallel rotations is provided, which is a special case of our Subproblem 2E. Subproblem 4 has been solved before as part of the solution to the inverse kinematics of a spherical wrist, such as in [24]. However, it does not seem to have been discussed in literature as its own subproblem for robot inverse kinematics. Although the papers discussed above have contributed solutions to Subproblems 1, 2, 2E, 3, and 5, we have not seen any literature discussing Subproblems 4 or 6, which appear to be new subproblems.

Our approach is to solve each subproblem as a parameterized solution of a linear least-squares problem involving sine

and cosine functions of unknown angles. We then impose the geometric constraint (the solution has to lie on a circle) on the family of solutions to find the least-squares solution. A similar approach was used in [25] to find the intersection of spheres which arises in the localization problem using multiple range sensors. It is one inspiration for our method of expressing a nonlinear least-squares problem as a linear problem, and then applying constraints to the set of linear solutions.

After providing the subproblem solutions, we describe how to apply these subproblems to the robot inverse kinematics problem. Subproblems 5 and 6 allow for solving some of the most general cases of robots with closed-form inverse kinematics. We show that these subproblems may be used to solve inverse kinematics of any 6R robot arm containing a spherical joint or three consecutive parallel axes, commonly referred to as the Pieper criterion. There is sometimes a misconception [26] that a robot with three intersecting or parallel joints but no other constraints does not have a closed-form inverse kinematics solution. But with Subproblems 5 and 6, these closed-form solutions do indeed exist. For robots that satisfy the Pieper criterion and have certain additional sets of parallel or intersecting axes, their inverse kinematics can be solved using just Subproblems 1, 2, 3, and 4. Since these subproblems are posed as least-squares minimizations, the inverse kinematics algorithm can find the least-squares solution for end effector poses outside of the workspace *without iteration*. For an arbitrary 6-dof arm, the analytical inverse kinematics solution does not exist in general, but the subproblems are still helpful in reducing the problem to a low-dimensional search.

We also present an evaluation of the computational performance of the subproblem and robot inverse kinematics solutions. These algorithms have been implemented in MATLAB and are available in a publicly accessible repository<sup>1</sup>.

## II. APPROACH

The subproblem solutions presented in this paper involve converting equations involving rotations into linear equations in  $x = [s_\theta \ c_\theta]^T$ , where  $s_\theta = \sin \theta$  and  $c_\theta = \cos \theta$ . These equations can be solved with the tools of linear algebra, and the  $\sin^2(\theta) + \cos^2(\theta) = \|x\|^2 = 1$  constraint can be imposed at the end. Once we obtain the constrained solution of  $x$ , we can find  $\theta = \text{ATAN2}(x_1, x_2)$ .

We will repeatedly use the Euler-Rodrigues formula [27], [28]:

$$R(k, \theta) = kk^T + s_\theta k^\times - c_\theta k^{\times 2}, \quad (1)$$

where  $k^\times$  denotes the matrix representation of the cross product. For  $k = [k_1, k_2, k_3]^T$ ,

$$k^\times := \begin{bmatrix} 0 & -k_3 & k_2 \\ k_3 & 0 & -k_1 \\ -k_2 & k_1 & 0 \end{bmatrix}, \quad (2)$$

and  $k^{\times 2} = k^\times k^\times = kk^T - I$ . To convert a problem involving rotations to a linear problem, we use (1) to write

$$R(k, \theta)p = p_k + A_{k,p}x, \quad (3)$$

where

$$p_k = kk^T p, \quad (4)$$

and

$$A_{k,p} = \begin{bmatrix} k^\times p & -k^{\times 2} p \end{bmatrix}. \quad (5)$$

Geometrically, this conversion from rotations to linear equations in  $x = [s_\theta \ c_\theta]^T$  can be viewed as replacing any circle of the top of a cone with the plane in which the circle lies.  $p_k$  is the vector along the center of the cone pointing to the top of the cone, and  $A_{k,p}$  is a basis for the plane in which the top of the cone lies. The columns of  $A_{k,p}$  are orthogonal and have norm equal to the radius of the top of the cone. After finding the solutions within this plane, we can then constrain the solutions to just those lying on the circle.

To solve a subproblem, we can use (3) to substitute any rotation with a linear expression in  $x$ . The resulting linear equation may have many solutions, one solution, or no solution. Among these solutions, only some of them may satisfy the  $\|x\|^2 = 1$  constraint.

If the unconstrained linear equation  $Ax = b$  has many solutions, then its solutions can be parameterized as  $x = A^+x + x_N$ , where  $A^+ = A^T(AA^T)^{-1}$  (for  $A$  with full row rank) is the pseudo-inverse (right inverse) of  $A$ , and  $x_N$  is an arbitrary vector in the null space of  $A$ . If the null space is of dimension  $m$ , then we can parameterize  $x_N = \xi_1 x'_{N_1} + \dots + \xi_m x'_{N_m}$ , where  $x'_{N_i}$  forms a basis for the null space and  $\xi_i$  parameterizes the solution. Notice that  $x_{\min} = A^+x$  is the minimum-norm solution to the linear equation. If  $A$  has a null space of dimension one and  $x = [s_\theta \ c_\theta]^T$ , then we can use  $\|x\|^2 = 1$  to find  $\xi$  as the solution to a quadratic equation. If  $A$  has a null space of dimension two and  $x = [x_1^T \ x_2^T]^T = [s_{\theta_1} \ c_{\theta_1} \ s_{\theta_2} \ c_{\theta_2}]^T$ , then writing out  $\|x_1\|^2 = \|x_2\|^2 = 1$  results in the intersection of two ellipses with unknowns  $\xi_1$  and  $\xi_2$ . This intersection can then be solved by finding the roots of a quartic polynomial, which has a closed-form solution.

If the unconstrained linear equation has no solutions, then we can solve for  $x_{LS} = \arg \min_x \|Ax - b\| = A^+b$ , where  $A^+ = (A^T A)^{-1} A^T$  is the pseudo-inverse (left inverse) of  $A$  (for  $A$  with full column rank).

If the linear equation does not have any solution that satisfies  $\|x\|^2 = 1$ , then we can solve the constrained problem  $\min \|Ax - b\|$  using the Lagrange multiplier technique. Conveniently, the solution to the constrained problem is often related to  $x_{\min}$  or  $x_{LS}$ . Geometrically, this often is the case because the closest point to a circle on a plane is the intersection of the circle and the ray from the center of the circle which passes through the point.

Much of the work in the following subproblem solutions involves finding computationally efficient expressions for  $A^+$ ,  $x'_{N_i}$  and  $\xi_i$ . Some extra computational speed-up can also be achieved by recognizing that  $\text{ATAN2}(s_\theta, c_\theta) = \text{ATAN2}(\alpha s_\theta, \alpha c_\theta)$  where  $\alpha > 0$ . This means we only have to solve for  $\alpha x$ .

<sup>1</sup><https://github.com/rpiRobotics/linear-subproblem-solutions>

### III. SUBPROBLEM SOLUTIONS

#### SUBPROBLEM 1: CONE AND POINT

Given vectors  $p_1$ ,  $p_2$  and a unit vector  $k$ , find  $\theta$  to minimize  $\|R(k, \theta)p_1 - p_2\|$ .

Without loss of generality, assume  $k$  and  $p_1$  are not collinear, and assume  $k$  and  $p_2$  are not collinear. Otherwise,  $\theta$  is arbitrary. Using (3), we have

$$\|R(k, \theta)p_1 - p_2\| = \|A_{k,p_1}x - p\| \quad (6)$$

where

$$p = p_2 - p_{1k} = p_2 - kk^T p_1. \quad (7)$$

Note that by assumption,  $A_{k,p_1}$  is of full column rank. An exact solution to  $A_{k,p_1}x = p$  such that  $\|x\| = 1$  exists when  $\|p_1\| = \|p_2\|$  and  $k^T p_1 = k^T p_2$ , or, equivalently,  $\|k^\times p_1\| = \|k^\times p_2\|$  and  $k^T p_1 = k^T p_2$ . If these conditions are satisfied, then

$$x = A_{k,p_1}^+ p. \quad (8)$$

Furthermore, one can show that  $A_{k,p_1}^T A_{k,p_1} = \|k^\times p_1\|^2 \cdot I$  and  $A_{k,p_1}^+ = \frac{A_{k,p_1}^T}{\|k^\times p_1\|^2}$ . Because of the condition  $k^T p_1 = k^T p_2$ ,  $p$  lies in the range space of  $A_{k,p_1}$  and  $A_{k,p_1}x = A_{k,p_1}A_{k,p_1}^+ p = p$ . Under the condition  $\|p_1\| = \|p_2\|$  or equivalently  $\|k^\times p_1\| = \|k^\times p_2\|$ , we satisfy the constraint  $\|x\| = 1$ .

In general, an exact solution is not possible, and we need to solve the constrained least-squares problem  $\min_x \|A_{k,p_1}x - p\|$  subject to  $\|x\| = 1$ . By using the Lagrange multiplier  $\lambda$  to enforce the equality constraint, the solution is given by

$$x = (\lambda I + A_{k,p_1}^T A_{k,p_1})^{-1} A_{k,p_1}^T p, \quad (9)$$

where  $\lambda$  is chosen so that  $\|x\| = 1$ . Since we know  $A_{k,p_1}^T A_{k,p_1} = \|k^\times p_1\|^2 \cdot I$ , the optimal solution simplifies to

$$x = \frac{A_{k,p_1}^T p}{\lambda + \|k^\times p_1\|^2}. \quad (10)$$

This means  $\left| \lambda + \|k^\times p_1\|^2 \right| = \left\| A_{k,p_1}^T p \right\|$ . The two solutions of  $\lambda$  correspond to the maximizing and minimizing solutions of the constrained least-squares problem. For the minimizing solution,  $\lambda + \|k^\times p_1\|^2 > 0$ . Therefore, the least-squares solution is

$$x = \frac{A_{k,p_1}^T p}{\left\| A_{k,p_1}^T p \right\|}. \quad (11)$$

The value of ATAN2 does not change with equal positive scaling of its inputs, so we can skip the scalar division. We can also use the simplification  $A_{k,p_1}^T p = A_{k,p_1}^T p_2$  and arrive at the solution

$$\theta = \text{ATAN2}((k^\times p_1)^T p_2, -(k^\times p_1)^T p_2). \quad (12)$$

The solution may also be viewed geometrically, as shown in Fig. 1. The unconstrained solution  $x_{LS} = \min_x \|A_{k,p_1}x - p\|$  is the coordinates in the coordinate system  $(-k^\times p_1, k^\times p_1)$

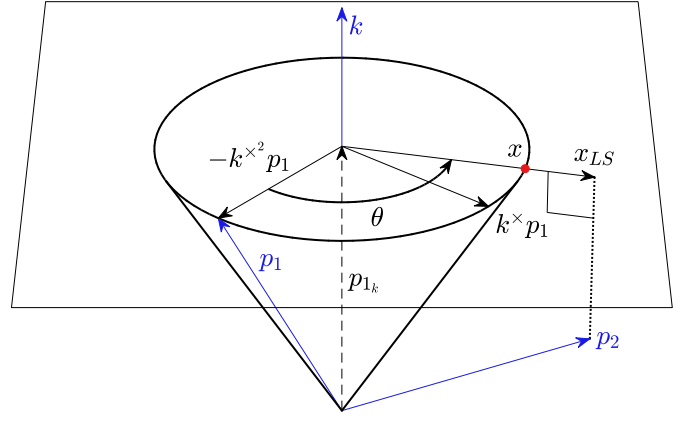


Fig. 1. Subproblem 1 finds the angle of the closet point on the cone  $R(k, \theta)p_1$  to the point  $p_2$ . This is the angle of  $x_{LS}$  in the coordinate frame at the top of the cone formed by  $(-k^\times p_1, k^\times p_1)$ , where  $x_{LS}$  is the projection of  $p_2$  to the plane along the top of the cone.

of  $p_2$  projected onto the plane containing the top of the cone. The closest point on a circle to some point on the same plane is that point scaled to the circle's radius. This means we can use  $x_{LS}$  to find the angle between  $p_1$  and the closest point on the cone to  $p_2$ .

#### SUBPROBLEM 2: TWO CONES

Given vectors  $p_1$ ,  $p_2$  and unit vectors  $k_1$ ,  $k_2$ , find  $(\theta_1, \theta_2)$  to minimize  $\|R(k_1, \theta_1)p_1 - R(k_2, \theta_2)p_2\|$ .

Without loss of generality, assume the follow pairs of vectors are not collinear:  $(k_1, p_1)$ ,  $(k_2, p_2)$ ,  $(k_1, k_2)$ . Otherwise, the problem either reduces to the Subproblem 1 or  $(\theta_1, \theta_2)$  are arbitrary.

Notice that an exact solution  $R(k_1, \theta_1)p_1 = R(k_2, \theta_2)p_2$  is possible only if  $\|p_1\| = \|p_2\|$ , as this guarantees the top of the two cones lie on the same sphere. Otherwise, we can find the least-squares solution by rescaling  $p_1$  and  $p_2$  to the same length before proceeding, such as by normalizing them. We will solve the subproblem assuming  $\|p_1\| = \|p_2\|$ , and then show that rescaling  $p_1$  and  $p_2$  to the same length gives the least-squares solution.

Applying (3), we obtain

$$R(k_1, \theta_1)p_1 - R(k_2, \theta_2)p_2 = Ax - p, \quad (13)$$

where

$$A = [A_{k_1,p_1} \quad A_{k_2,p_2}], \text{ and } p = p_{2k} - p_{1k}. \quad (14)$$

As we have eliminated the degenerate cases,  $A$  is full rank and has a one-dimensional null space. The complete solution of  $x$  is

$$x = x_{min} + x_N \quad (15)$$

where  $x_{min} = A^+ p$  is the unconstrained minimum-norm solution,  $A^+ = A^T(AA^T)^{-1}$ , and  $x_N$  any vector in the one-dimensional null space of  $A$ . Although  $x_{min}$  and  $x_N$  may be computed numerically from  $A$  and  $p$ , we can achieve a

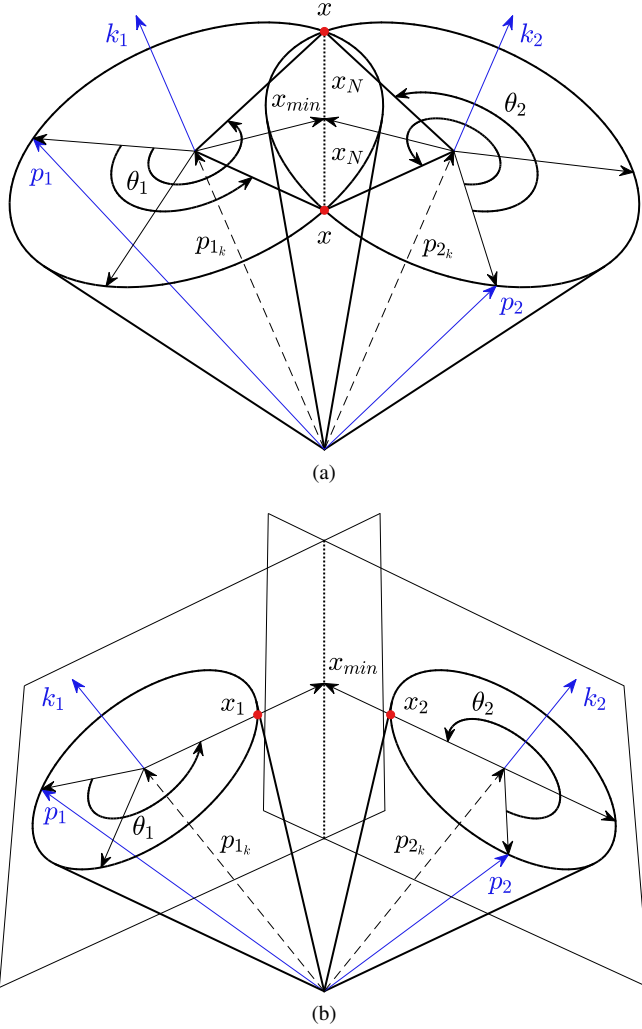


Fig. 2. Subproblem 2 finds the angles of the closest points on the two cones  $R(k_1, \theta_1)p_1$  and  $R(k_2, \theta_2)p_2$ . (a) Two intersecting cones with two intersection points. The solutions are found along the intersection of the planes along the top of the two cones. (b) Two non-intersecting cones. The minimizing solution is the angle of the minimum-norm point on the intersection of the two planes along the top of the cones.

computational speedup by taking advantage of the structure of  $A$ , as we will show below.

Geometrically, we can visualize the complete solution as the intersection between the two planes enclosing the top of the two cones, as shown in Fig. 2. The intersection of the two planes is a line in the direction  $k_1^\times k_2$ . The unconstrained minimum-norm solution  $x_{min}$  is given by the intersection of this line and the plane of symmetry containing  $k_1$  and  $k_2$ .

It follows that

$$A_{k_1, p_1} x_{min_1} + p_{1k} = A_{k_2, p_2} x_{min_2} + p_{2k} = \alpha_1 k_1 + \alpha_2 k_2, \quad (16)$$

where  $(\alpha_1, \alpha_2)$  are constants. Projecting these equations onto  $k_1$  and  $k_2$ , we can solve for  $(\alpha_1, \alpha_2)$ :

$$\begin{bmatrix} \alpha_1 \\ \alpha_2 \end{bmatrix} = \frac{1}{1 - (k_1^T k_2)^2} \begin{bmatrix} k_1^T p_1 - k_1^T k_2 k_2^T p_2 \\ k_2^T p_2 - k_1^T k_2 k_1^T p_1 \end{bmatrix}. \quad (17)$$

From (16), we can solve for  $x_{min}$ :

$$\begin{aligned} x_{min_1} &= A_{k_1, p_1}^+ (\alpha_1 k_1 + \alpha_2 k_2) = \alpha_2 A_{k_1, p_1}^+ k_2 \\ x_{min_2} &= A_{k_2, p_2}^+ (\alpha_1 k_1 + \alpha_2 k_2) = \alpha_1 A_{k_2, p_2}^+ k_1 \end{aligned} \quad (18)$$

where  $A_{k_i, p_i}^+ = \frac{A_{k_i, p_i}^T}{\|k_i^\times p_i\|^2}$  as in Subproblem 1.

To efficiently calculate  $x_N$ , we can represent the line spanned by  $k_1^\times k_2$  in the  $A_{k_1, p_1}$ ,  $A_{k_2, p_2}$  coordinate systems as

$$A_{k_1, p_1} x_{N_1} = A_{k_2, p_2} x_{N_2} = \xi k_1^\times k_2, \quad (19)$$

where  $\xi$  is an arbitrary constant. It follows that

$$x_N = \xi \begin{bmatrix} x'_{N_1} \\ x'_{N_2} \end{bmatrix}, \quad x'_{N_1} = A_{k_1, p_1}^+ k_1^\times k_2, \quad x'_{N_2} = A_{k_2, p_2}^+ k_1^\times k_2. \quad (20)$$

The complete solution  $x$  in (15) may now be written as

$$x = x_{min} + x_N = \begin{bmatrix} x_{min_1} + \xi x'_{N_1} \\ x_{min_2} + \xi x'_{N_2} \end{bmatrix}. \quad (21)$$

Note that  $x_{min_i}^T x'_{N_i} = 0$ .

Now that we have found the unconstrained least-squares solution, we can introduce the  $\|x_i\| = 1$  constraint to find  $x$ . There are three possible cases:

- 1)  $\|x_{min_i}\| < 1$ : The two cones intersect at two points. Since  $\|x_i\| = 1$ , we can solve for  $\xi$ :

$$\xi = \pm \frac{\sqrt{1 - \|x_{min_i}\|^2}}{\|x'_{N_i}\|}. \quad (22)$$

Note that  $\xi$  is the same for both  $i = 1, 2$ . In this case,  $x_{min}$  corresponds to an interior point of both cones, and the points of intersection are in the  $\pm k_1^\times k_2$  directions, as shown in Fig. 2(a).

- 2)  $\|x_{min_i}\| = 1$ : The two cones intersect at exactly one point. The solution is just the least-squares solution  $x = x_{min}$ .
- 3)  $\|x_{min_i}\| > 1$ : The two cones do not intersect. We need to solve the least-squares problem subject to the equality constraints  $\|x_i\|^2 = 1$ ,  $i = 1, 2$ . Using the Lagrange multiplier approach to enforce the equality constraints, we need to find  $(\lambda_1, \lambda_2)$  so that

$$\begin{aligned} x_1 &= (\lambda_1 I + A_{k_1, p_1}^T A_{k_1, p_1})^{-1} A_{k_1, p_1}^T (p - A_{k_2, p_2} x_2) \\ x_2 &= (\lambda_2 I + A_{k_2, p_2}^T A_{k_2, p_2})^{-1} A_{k_2, p_2}^T (p - A_{k_1, p_1} x_1). \end{aligned} \quad (23)$$

with  $(\lambda_1, \lambda_2)$  chosen so that  $\|x_1\| = \|x_2\| = 1$ . It may be shown that the solution for  $x_i$  is the scaled version of  $x_{min_i}$ , that is,  $x_i = x_{min_i} / \|x_{min_i}\|$ .

Once the solution  $x$  is found (Two solutions in case 1, one solution in cases 2 and 3), the corresponding solution of Subproblem 2 is:

$$\theta_1 = \text{ATAN2}(x_1^{(1)}, x_1^{(2)}), \quad \theta_2 = \text{ATAN2}(x_2^{(1)}, x_2^{(2)}) \quad (24)$$

where  $x_i^{(j)}$  is the  $j$ th element of  $x_i$ . Recall that ATAN2 is unaffected by positive scaling of its inputs, which means that in case 3 we can skip the scalar division and directly plug in  $x_{min}$ .

All there is left to show is that the cases above yield the least-squares solution(s) if  $\|p_1\| \neq \|p_2\|$ , and these vectors were scaled to the same length before using the solution above. We can rewrite the subproblem as

$$\begin{aligned} & \|R(k_1, \theta_1)p_1 - R(k_2, \theta_2)p_2\|^2 \\ &= \|p_1\|^2 + \|p_2\|^2 - 2\|p_1\|\|p_2\|\cos(\psi), \end{aligned} \quad (25)$$

where the cosine of the angle between rotated vectors is

$$\cos(\psi) = \left( R(k_1, \theta_1) \frac{p_1}{\|p_1\|} \right)^T R(k_2, \theta_2) \frac{p_2}{\|p_2\|}. \quad (26)$$

We see that the minimizing  $(\theta_1, \theta_2)$  is independent of  $\|p_1\|$  and  $\|p_2\|$ .

#### SUBPROBLEM 2 EXTENDED: TWO OFFSET CONES

Given vectors  $p_0, p_1, p_2$  and unit vectors  $k_1, k_2$ , find  $(\theta_1, \theta_2)$  to solve  $p_0 + R(k_1, \theta_1)p_1 = R(k_2, \theta_2)p_2$ .

This subproblem extension is the same as Subproblem 2 except the base of the two cones are shifted by a vector  $p_0$ , as shown in Fig. 3. Unlike Subproblem 2, the positions of the rotated  $p_1$  and  $p_2$  are not constrained to be on concentric spheres. There are three scalar equations and two unknowns, so the problem is generally unsolvable. In other words, with randomly chosen parameters, there is almost surely no solution for  $(\theta_1, \theta_2)$ . It is therefore inadvisable to use Subproblem 2E as part of the solution to a larger geometry problem, and we see that the robot inverse kinematics solutions presented later in this paper do not use Subproblem 2E. Despite this, many authors have discussed solutions to this modified subproblem in recent literature such as [5], [7], [8], [15], [19], and so we present here a straightforward solution method.

We can use the same approach as Subproblem 2 to write the problem as  $Ax = p$  subject to  $\|x_1\| = \|x_2\| = 1$ , where  $A$  and  $x$  are as in (14), and  $p$  is modified to be

$$p = p_{2k} - p_{1k} - p_0. \quad (27)$$

Since  $A$  is the same as in Subproblem 2, the null space is given by (20). The unconstrained minimum-norm solution is still  $x_{min} = A^+p$ , but  $A_{k_1, p_1}x_{min_1} + p_{1k} + p_0$  and  $A_{k_2, p_2}x_{min_2} + p_{2k}$  no longer lie in a plane of symmetry (which does not exist in general).

Although we cannot use (16) in this case, there is still a small computational advantage to gain over numerically computing  $x_{min}$ . Notice that

$$\begin{aligned} AA^T &= A_{k_1, p_1}A_{k_1, p_1}^T + A_{k_2, p_2}A_{k_2, p_2}^T \\ &= \|k_1^\times p_1\|^2 (I - k_1 k_1^T) + \|k_2^\times p_2\|^2 (I - k_2 k_2^T) \\ &= (\|k_1^\times p_1\|^2 + \|k_2^\times p_2\|^2) \underbrace{(I - \alpha k_1 k_1^T - \beta k_2 k_2^T)}_M, \end{aligned} \quad (28)$$

where

$$\alpha = \frac{\|k_1^\times p_1\|^2}{\|k_1^\times p_1\|^2 + \|k_2^\times p_2\|^2}, \quad \beta = \frac{\|k_2^\times p_2\|^2}{\|k_1^\times p_1\|^2 + \|k_2^\times p_2\|^2}. \quad (29)$$

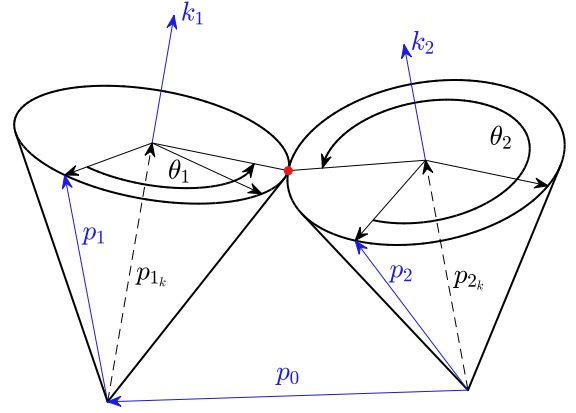


Fig. 3. Subproblem 2E finds the angles of intersection between the offset cone  $p_0 + R(k_1, \theta_1)p_1$  and the cone  $R(k_2, \theta_2)p_2$ .

This means that  $AA^T$  is a scaled sum of the identity matrix with two rank-one matrices, which we can use to speed up computation. Iteratively applying the Woodbury matrix identity, which in this case is also the Sherman–Morrison formula, we see that

$$M^{-1} = I + k_1 k_1^T \frac{\alpha}{1 - \alpha}, \quad (30)$$

and

$$(AA^T)^{-1} = \frac{M^{-1} + \frac{M^{-1}k_2 k_2^T M^{-1}\beta}{1 - k_2^T M^{-1}k_2 \beta}}{\|k_1^\times p_1\|^2 + \|k_2^\times p_2\|^2}. \quad (31)$$

We can then compute

$$x_{min} = A^T (AA^T)^{-1} p. \quad (32)$$

Once we calculate  $x_{min}$  either numerically or using the iterative method above, the general solution is

$$x = x_{min} + \xi x'_{N_1}. \quad (33)$$

The two normality conditions  $\|x_1\| = 1$  and  $\|x_2\| = 1$  result in two quadratic equations in  $\xi$ :

$$\xi^2 + 2 \frac{x_{min_1}^T x'_{N_1}}{\|x'_{N_1}\|^2} \xi + \frac{\|x_{min_1}\|^2 - 1}{\|x'_{N_1}\|^2} = 0 \quad (34)$$

for  $i = 1, 2$ . In the unmodified Subproblem 2,  $x_{min_i}^T x_{N_i} = 0$ . This is no longer the case in general if  $p_0 \neq 0$ . In that case, we can solve for a unique solution of  $\xi$ :

$$\xi = \frac{1}{2} \frac{(\|x_{min_2}\|^2 - 1) \|x'_{N_1}\|^2 - (\|x_{min_1}\|^2 - 1) \|x'_{N_2}\|^2}{x_{min_1}^T x'_{N_1} \|x'_{N_2}\|^2 - x_{min_2}^T x'_{N_2} \|x'_{N_1}\|^2}. \quad (35)$$

The angles  $\theta_i$  are then solved from  $\theta_i = \text{ATAN2}(x_i^{(1)}, x_i^{(2)})$ . Note that (35) only finds the shared zeros of (34) when they exist. Therefore, we need to plug  $\xi$  back into (34) to determine if the cones intersect.

When  $p_0$  lies in the plane of  $k_1$  and  $k_2$ , we can write  $p_0$  in terms of rotations about  $k_1$  and  $k_2$  as

$$p_0 = a_1 k_1 + a_2 k_2 = R(k_1, \theta_1) a_1 k_1 + R(k_2, \theta_2) a_2 k_2. \quad (36)$$

Then the minimum-norm problem becomes a special case of Subproblem 2:

$$\min_{\theta_1, \theta_2} \|\mathbf{R}(k_1, \theta_1)(p_1 + a_1 k_1) - \mathbf{R}(k_2, \theta_2)(p_2 - a_2 k_2)\|. \quad (37)$$

Another Subproblem 2 scenario involves solving for intersections between two cones when  $k_1 = k_2 = k$ :

$$\min_{\theta_1, \theta_2} \|p_0 + \mathbf{R}(k, \theta_1)p_1 - \mathbf{R}(k, \theta_2)p_2\|. \quad (38)$$

In this case, we require  $k^T(p_0 + p_1 - p_2) = 0$  to guarantee exact solutions. Up to two solutions of  $\theta_1$  may be solved using Subproblem 3, and the corresponding solutions of  $\theta_2$  using Subproblem 1. Note that we can rewrite

$$\begin{aligned} & \|p_0 + \mathbf{R}(k, \theta_1)p_1 - \mathbf{R}(k, \theta_2)p_2\|^2 \\ &= \left\| -k^{\times 2} p_0 + \mathbf{R}(k, \theta_1)(-k^{\times 2} p_1) - \mathbf{R}(k, \theta_2)(-k^{\times 2} p_2) \right\|^2 \\ & \quad + \|p_{0k} + p_{1k} - p_{2k}\|^2. \end{aligned} \quad (39)$$

This means we find up to two least-squares solutions if  $k^T(p_0 + p_1 - p_2) \neq 0$  by replacing  $p_i$  with  $-k^{\times 2} p_i$ .

### SUBPROBLEM 3: CONE AND SPHERE

Given vectors  $p_1, p_2$ , a unit vector  $k$ , and a positive scalar  $d$ , find  $\theta$  to minimize  $\|\mathbf{R}(k, \theta)p_1 - p_2\| - d$ .

Without loss of generality, assume  $k$  and  $p_1$  are not collinear, and assume  $k$  and  $p_2$  are not collinear; otherwise, the problem is independent of  $\theta$ . Write the problem equivalently as minimizing  $\left| \|\mathbf{R}(k, \theta)p_1 - p_2\|^2 - d^2 \right|$ . Applying (3), we get

$$\begin{aligned} & \|\mathbf{R}(k, \theta)p_1 - p_2\|^2 - d^2 \\ &= \|p_{1k} - p_2\|^2 - 2p_2^T A_{k,p_1} x + x^T A_{k,p_1}^T A_{k,p_1} x - d^2 \quad (40) \\ &= \|p_{1k} - p_2\|^2 - 2p_2^T A_{k,p_1} x + \|k^{\times} p_1\|^2 - d^2. \end{aligned}$$

Note that we have used the fact that  $A_{k,p_1}^T A_{k,p_1} = \|k^{\times} p_1\|^2 I_2$ , and  $\|x\| = 1$ . By factoring out a constant, Subproblem 3 may be written as the minimization of  $|p_2^T A_{k,p_1} x - b|$ , where

$$b = \frac{1}{2} \|p_{1k} - p_2\|^2 + \frac{1}{2} \|k^{\times} p_1\|^2 - \frac{d^2}{2}. \quad (41)$$

By assumption, the  $2 \times 1$  row vector  $p_2^T A_{k,p_1}$  is of rank one and has a one-dimensional null space given by  $p_2^T A_{k,p_1} x_N = 0$ , where

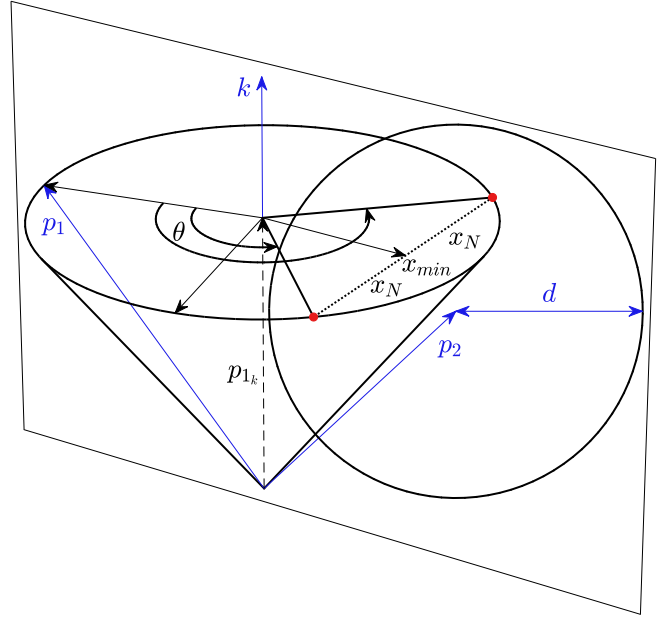
$$x_N = \xi x'_N, \quad x'_N = \begin{bmatrix} 0 & 1 \\ -1 & 0 \end{bmatrix} A_{k,p_1}^T p_2. \quad (42)$$

Geometrically, the null space is the intersection between the plane containing the top of the cone (range of  $A_{k,p_1}$ ) and a plane perpendicular to  $p_2$ . The minimum-norm solution  $x_{min}$  is given by

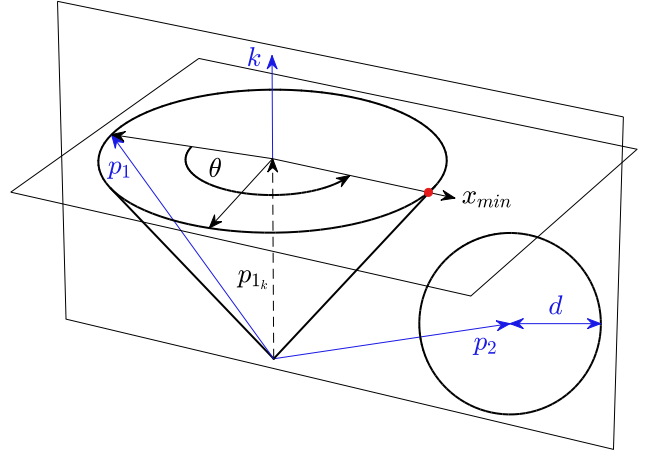
$$x_{min} = \frac{A_{k,p_1}^T p_2}{\|A_{k,p_1}^T p_2\|^2} b \quad (43)$$

which is along the intersection of the top of the cone and the plane of symmetry spanned by  $k$  and  $p_2$ . The complete solution is then given by

$$x = x_{min} + \xi x'_N. \quad (44)$$



(a)



(b)

Fig. 4. Subproblem 3 finds the angles of the closest points on the cone  $\mathbf{R}(k, \theta)p_1$  to the sphere of radius  $d$  centered at  $p_2$ . (a) Intersecting cone and sphere. (b) Minimum distance between a non-intersecting cone and sphere.

Note that  $x_{min}$  and  $x'_N$  are orthogonal. There are three cases, of which cases 1 and 3 are shown in Fig. 4:

- 1)  $\|x_{min}\| < 1$ : The cone intersects with the sphere at two points. Since  $\|x\| = 1$ , we have

$$\xi = \pm \frac{\sqrt{1 - \|x_{min}\|^2}}{\|x'_N\|} = \pm \frac{\sqrt{\|A_{k,p_1}^T p_2\|^2 - b^2}}{\|A_{k,p_1}^T p_2\|^2}. \quad (45)$$

The two feasible solutions are  $x = x_{LS} + \xi x'_N$ .

- 2)  $\|x_{min}\| = 1$ : The cone intersects exactly once with the sphere. The one feasible solution is  $x = x_{min}$ .
- 3)  $\|x_{min}\| > 1$ : The cone and sphere do not intersect. We need to solve the constrained least-squares problem by finding  $\lambda$  so that  $x = (\lambda I + A_{k,p_1}^T p_2 p_2^T A_{k,p_1})^{-1} A_{k,p_1}^T p_2 b$  has unit norm. With a little algebra, we can show  $x$  is



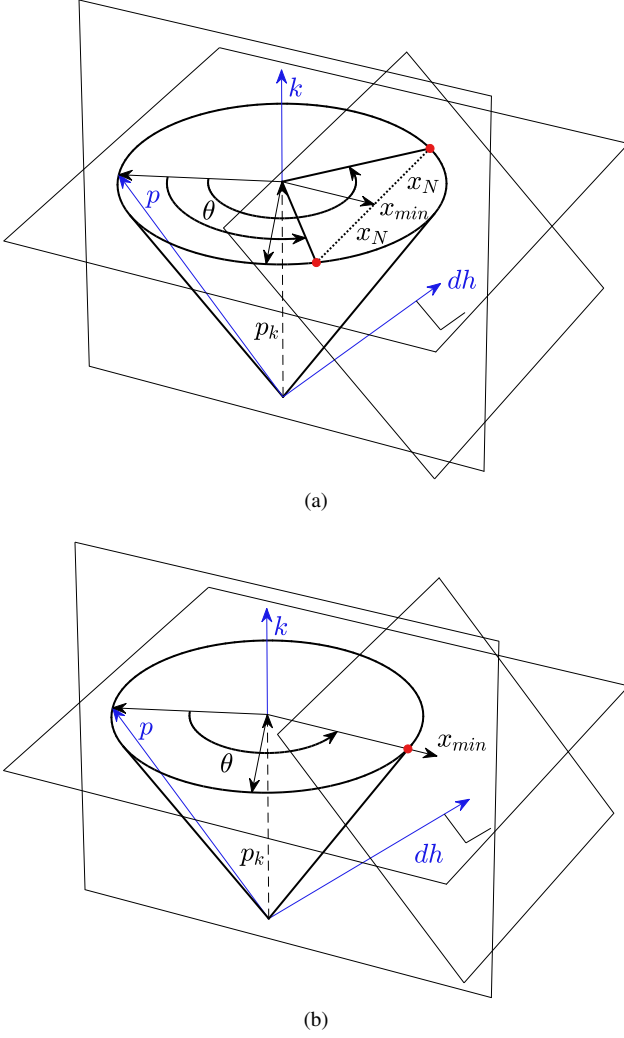


Fig. 5. Subproblem 4 finds the angles of the closest points on the cone  $R(k, \theta)p$  to the plane with normal vector  $h$  and distance  $d$  from the origin. (a) A cone intersecting with a shifted plane. (b) Minimum distance between non-intersecting cone and plane.

just  $A_{k,p_1}^T p_2$  scaled by a constant. In this case,

$$x = \frac{A_{k,p_1}^T p_2}{\|A_{k,p_1}^T p_2\|}. \quad (46)$$

In each case, once  $x = [x_1, x_2]^T$  is found, the corresponding  $\theta$  that solves Subproblem 3 is given by

$$\theta = \text{ATAN2}(x_1, x_2). \quad (47)$$

Recall that ATAN2 is unaffected by positive scaling of its inputs, which means that in case 3 we can skip the scalar division and directly plug in  $x_{min}$ .

#### SUBPROBLEM 4: CONE AND PLANE

Given a vector  $p$ , unit vectors  $k$ ,  $h$ , and a scalar  $d$ , find  $\theta$  to minimize  $|h^T R(k, \theta)p - d|$ .

Without loss of generality, assume  $p$  and  $k$  are not collinear, and assume  $h$  and  $k$  are not collinear; otherwise, the problem does not depend on  $\theta$ . If we apply (3), then

$$h^T R(k, \theta)p - d = h^T A_{k,p} x - b \quad (48)$$

where

$$b = d - h^T k k^T p. \quad (49)$$

By assumption, the  $2 \times 1$  row vector  $h^T A_{k,p}$  is of rank one and has a one-dimensional null space given by  $h^T A_{k,p} x_N = 0$ , where

$$x_N = \xi x'_N, \quad x'_N = \underbrace{\begin{bmatrix} 0 & 1 \\ -1 & 0 \end{bmatrix}}_J A_{k,p}^T h. \quad (50)$$

The null space is the intersection between the plane containing the top of the cone and a plane perpendicular to  $h$ . The minimum-norm solution  $x_{min}$  is given by

$$x_{min} = \frac{A_{k,p}^T h}{\|A_{k,p}^T h\|^2} b \quad (51)$$

which is the point of intersection among three planes: The plane spanned by the top of the cone, the plane perpendicular to  $dh$ , and the plane of symmetry spanned by  $k$  and  $h$ . The complete solution is

$$x = x_{min} + \xi x'_N \quad (52)$$

where  $x_{min}$  and  $x'_N$  are orthogonal.

As before, there are three possible cases:

- 1)  $\|x_{min}\| < 1$ : The cone intersects with the plane at two points. Since  $\|x\| = 1$ , we have

$$\xi = \pm \frac{\sqrt{1 - \|x_{min}\|^2}}{\|x'_N\|} = \pm \frac{\sqrt{\|A_{k,p}^T h\|^2 - b^2}}{\|A_{k,p}^T h\|^2}. \quad (53)$$

The two feasible solutions are  $x = x_{min} + \xi x'_N$ .

- 2)  $\|x_{min}\| = 1$ : The cone intersects with the plane at one point. The one feasible solution is given by  $x = x_{min}$ .
- 3)  $\|x_{min}\| > 1$ : The cone does not intersect with the plane. We need to solve the constrained least-squares problem by finding  $\lambda$  so that  $x = (\lambda I + A_{k,p}^T h h^T A_{k,p})^{-1} A_{k,p}^T h b$  has unit norm. With a little algebra, we can show  $x$  is just  $A_{k,p}^T h$  scaled by a constant. In this case,

$$x = \frac{A_{k,p}^T h}{\|A_{k,p}^T h\|}. \quad (54)$$

In each case, once  $x = [x_1, x_2]^T$  is found, the corresponding  $\theta$  that solves Subproblem 4 is given by

$$\theta = \text{ATAN2}(x_1, x_2). \quad (55)$$

Since ATAN2 is not affected by positive scaling of its inputs, we can skip the scalar division in case 3 and directly use  $A_{k,p}^T h$ . Visualizations of cases 1 and 3 of Subproblem 4 are shown in Fig. 5.

**SUBPROBLEM 5: THREE CONES**

Given vectors,  $p_0, p_1, p_2, p_3$  and unit vectors  $k_1, k_2, k_3$ , find  $(\theta_1, \theta_2, \theta_3)$  to solve

$$p_0 + R(k_1, \theta_1)p_1 = R(k_2, \theta_2)(p_2 + R(k_3, \theta_3)p_3). \quad (56)$$

We may visualize this subproblem as the intersection of three cones, as depicted in Fig. 6:

- Cone 1 is a shifted cone given by  $p_0 + R(k_1, \theta_1)p_1$ .
- Cone 2 rotates about  $k_2$  with radius  $r$  and height  $z$  to be determined, where  $z$  may be negative if the cone extends in the  $-k_2$  direction.
- Cone 3 is a shifted cone given by  $p_2 + R(k_3, \theta_3)p_3$ .

We will show that this subproblem can be reduced to finding the intersections between two ellipses, which in turn can be reduced to finding the roots of a quartic polynomial.

Without loss of generality, assume the pairs of vectors  $(k_1, p_1)$  and  $(k_3, p_3)$  are not collinear, as otherwise  $\theta_1$  or  $\theta_3$  is arbitrary. The projection of the solutions on cone 1 and cone 3 to  $k_2$  is  $z$ :

$$z = k_2^T(p_0 + R(k_1, \theta_1)p_1) = k_2^T(p_2 + R(k_3, \theta_3)p_3). \quad (57)$$

Write

$$\begin{aligned} p_0 + R(k_1, \theta_1)p_1 &= A_{k_1, p_1}x_1 + p_{1S}, \\ p_2 + R(k_3, \theta_3)p_3 &= A_{k_3, p_3}x_3 + p_{3S}, \end{aligned} \quad (58)$$

where the shifted centers of the cones are

$$p_{1S} = p_0 + k_1 k_1^T p_1, \quad p_{3S} = p_2 + k_3 k_3^T p_3. \quad (59)$$

Use Subproblem 4 to find  $x_1$  and  $x_3$  in terms of  $z$ :

$$x_i = \frac{v_i(z - \delta_i) \pm J v_i \sqrt{\|v_i\|^2 - (z - \delta_i)^2}}{\|v_i\|^2}, \quad (60)$$

where  $J$  is defined in (50),  $v_i = A_{k_i, p_i}^T k_2$ , and  $\delta_i = k_2^T p_{iS}$ . Project the cone 1 and cone 3 solutions to the plane containing the top of cone 2. They should have the same distance, which is the radius of cone 2:

$$r^2 = \|A_{k_i, p_i}x_i + p_{iS} - z k_2\|^2. \quad (61)$$

By substituting in (60) and simplifying terms, we obtain

$$\begin{aligned} \|A_{k_i, p_i}x_i + p_{iS} - z k_2\|^2 &= -z^2 - 2\alpha_i z \\ &\quad + \|k_i^\times p_i\|^2 + \|p_{iS}\|^2 + 2\alpha_i \delta_i \\ &\quad \pm 2\beta_i \sqrt{\|k_i^\times p_i\|^2 \|k_i^\times k_2\|^2 - (z - \delta_i)^2}, \end{aligned} \quad (62)$$

where

$$\alpha_1 = \frac{p_0^T k_1^\times k_2}{\|k_1^\times k_2\|^2}, \quad \alpha_3 = \frac{p_2^T k_3^\times k_2}{\|k_3^\times k_2\|^2}, \quad (63)$$

and

$$\beta_1 = \frac{p_0^T k_1^\times k_2}{\|k_1^\times k_2\|^2}, \quad \beta_3 = \frac{p_2^T k_3^\times k_2}{\|k_3^\times k_2\|^2}. \quad (64)$$

To arrive at (62), we have used

$$A_{k_i, p_i} J A_{k_i, p_i}^T = \|k_i^\times p_i\|^2 k_i^\times, \quad (65)$$

$$\|A_{k_i, p_i}^T k_2\|^2 = \|k_i^\times p_i\|^2 \|k_i^\times k_2\|^2, \quad (66)$$

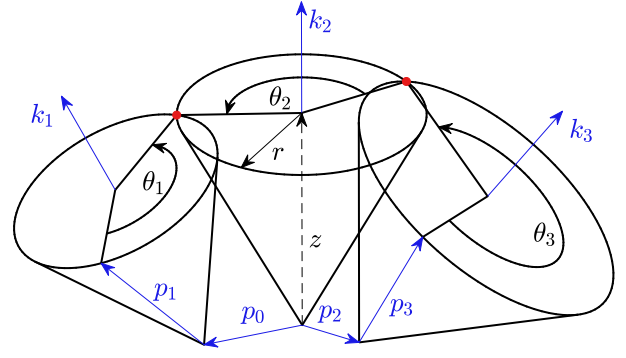


Fig. 6. Subproblem 5 finds the angles of intersections among three cones, where the height  $z$  and radius  $r$  of cone 2 are to be determined and depend on  $\theta_1$  and  $\theta_2$ . Note that in scenario depicted here, there exist other solutions of  $(\theta_1, \theta_2, \theta_3)$  associated with different  $(z, r)$ .

and

$$A_{k_i, p_i} A_{k_i, p_i}^T = -\|k_i^\times p_i\|^2 k_i^\times. \quad (67)$$

Equating the two right-hand-side expressions in (62) and cancelling the  $z^2$  terms, we are solving for the intersection of two ellipses which represent the cross sections of the surfaces obtained by revolving cones 1 and 3 around  $k_2$ . The ellipses may have anywhere from zero to four intersections, and each intersection corresponds to a  $(z_i, r_i)$ . For a given  $(z_i, r_i)$ , we can find one solution of  $\theta_1$  and  $\theta_3$  using (60), and then use Subproblem 1 to find the corresponding  $\theta_2$ .

Algebraically, we are solving for the zeros of an expression containing affine terms in  $z$  and two radicals. This can be converted to a quartic polynomial by isolating each radical and squaring the equation for each radical. The real-valued solutions to this quartic are the  $z$  coordinates of the intersections. Note that in some cases multiple intersections may share the same value of  $z$ .

There is a special case where the solution procedure simplifies when  $p_0^T k_1^\times k_2 = 0$  or  $p_2^T k_3^\times k_2 = 0$ , meaning that  $p_0$  (or  $p_2$ ) can be written as a linear combination of  $k_1$  and  $k_2$  (or  $k_2$  and  $k_3$ ), or  $k_1$  (or  $k_3$ ) is collinear with  $k_2$ . In this case, the equation for one of the ellipses degenerates into a line segment. This means that the two ellipses may intersect multiple times for a single  $(z, r)$ . Geometrically, this condition happens whenever axes (1, 2) or (2, 3) are coplanar, meaning that revolving the top of cone 1 or 3 around  $k_2$  results in a segment of a sphere or plane. If two axes are parallel, rewrite the subproblem such that  $p_0 = 0$  (or  $p_2 = 0$ ) and use Subproblem 3 and then Subproblem 2 to find the four solutions. If two axes are parallel, use Subproblem 4 and then Subproblem 2 and Subproblem 1.

In [3], another subproblem is posed based on the distances from two points to a vector with two consecutive rotations applied to it: Given vectors  $p, p_1, p_2$ , unit vectors  $k_1, k_2$ , and positive scalars  $d_1, d_2$ , find  $(\theta_1, \theta_2)$  so that

$$\begin{aligned} \|p_1 - R(k_1, \theta_1)R(k_2, \theta_2)p\| &= d_1 \\ \|p_2 - R(k_1, \theta_1)R(k_2, \theta_2)p\| &= d_2. \end{aligned} \quad (68)$$

This may arise, for example, in finding the joint angles of a robot arm using two range sensors on the end effector of



the arm. The problem may be transformed to a special case of Subproblem 6 as follows. The two distance conditions in (68) corresponds to the intersection of two spheres, which is a shifted cone. Then, (68) is just the intersection of three cones, with the axes of two cones intersecting. As discussed earlier, the problem may be solved using Subproblem 3 and then Subproblem 2 to find up to four solutions.

#### SUBPROBLEM 6: FOUR CONES

Given vectors  $p_i$ , unit vectors  $k_i$ ,  $h_i$ ,  $i \in \{1, 2, 3, 4\}$ , and scalars  $d_1$ ,  $d_2$ , find  $(\theta_1, \theta_2)$  to solve

$$\begin{cases} h_1^T R(k_1, \theta_1) p_1 + h_2^T R(k_2, \theta_2) p_2 = d_1 \\ h_3^T R(k_3, \theta_1) p_3 + h_4^T R(k_4, \theta_2) p_4 = d_2. \end{cases} \quad (69)$$

This problem involves four cones defined by  $(k_i, p_i)$ , where each cone also has a direction vector  $h_i$ . The position on the cone gets projected onto the  $h_i$  direction to get a distance for that cone. These cones are coupled so that the sums of distances for cones (1, 2) and (3, 4) must equal  $(d_1, d_2)$ , and also coupled so that cones (1, 3) and (2, 4) have the same rotation angles  $(\theta_1, \theta_2)$ .

We can use (3) to rewrite the subproblem as

$$\begin{bmatrix} h_1^T A_{k_1, p_1} & h_2^T A_{k_2, p_2} \\ h_3^T A_{k_3, p_3} & h_4^T A_{k_4, p_4} \end{bmatrix} \begin{bmatrix} x_1 \\ x_2 \end{bmatrix} = Ax = b = \begin{bmatrix} b_1 \\ b_2 \end{bmatrix}, \quad (70)$$

where

$$\begin{aligned} b_1 &= d_1 - h_1^T k_1 k_1^T p_1 - h_2^T k_2 k_2^T p_2, \\ b_2 &= d_2 - h_3^T k_3 k_3^T p_3 - h_4^T k_4 k_4^T p_4. \end{aligned} \quad (71)$$

The subproblem will yield unique solutions only if  $A$  is full rank. The unconstrained solutions to this linear equation are in the form

$$x = x_{min} + \xi_1 x'_{N1} + \xi_2 x'_{N2}, \quad (72)$$

where  $x_{min} = A^+ b$  is the minimum-norm solution,  $x'_{N1}$  and  $x'_{N2}$  form a basis for the null space of  $A$ , and  $\xi_1$  and  $\xi_2$  are arbitrary real numbers.  $x_{min}$ ,  $x'_{N1}$ , and  $x'_{N2}$  can be found numerically.

If we impose the constraints  $\|x_1\| = 1$  and  $\|x_2\| = 1$ , we get two equations for ellipses in  $(\xi_1, \xi_2)$ . Like in Subproblem 5, the intersection of two ellipses can be found by finding the roots of a quartic polynomial. The real solutions for  $(\xi_1, \xi_2)$  can then be used to find solutions to  $(x_1, x_2)$ , and therefore two unknown angles with

$$\theta_1 = \text{ATAN2}(x_1^{(1)}, x_1^{(2)}), \quad \theta_2 = \text{ATAN2}(x_2^{(1)}, x_2^{(2)}). \quad (73)$$

Notice that the problem simplifies if  $h_i$  is parallel to  $k_i$  for some  $i$ . In this case, one of the equations in (69) reduces to Subproblem 4. After solving for one angle from that equation, the other equation can be solved by using Subproblem 4 again.

#### IV. APPLICATION TO ROBOT INVERSE KINEMATICS

Consider a six-dof articulated robot with all revolute joints as shown in Fig. 7. We use the product of exponentials convention for the robot forward kinematics: Let  $\mathcal{O}_0$  be the origin of the world frame, and let  $\mathcal{O}_i$ , where  $i = 1, \dots, 6$ , be

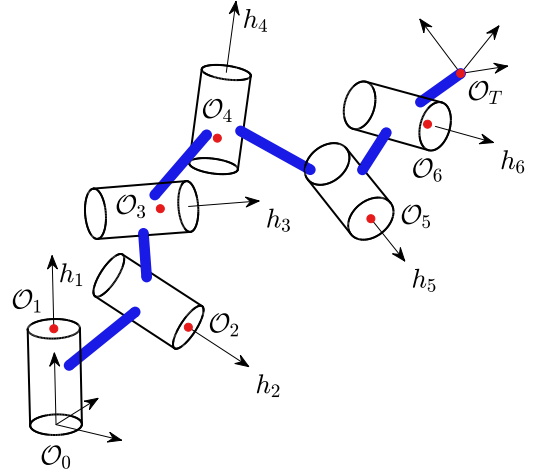


Fig. 7. General 6R robot arm with  $h_i$  as the  $i$ th joint axes and  $\mathcal{O}_i$  as the origin of frame  $i$ , placed anywhere along  $h_i$ . Inverse kinematics can be solved using Subproblem 5 and a 2D search over two of the joint angles.

the origin of frame  $i$ , placed anywhere along the  $i$ th joint axis, and where frame  $i$  has equal orientation to frame  $i - 1$  when joint  $i$  is in the zero configuration. Also let  $\mathcal{O}_T$  be the origin of the end effector tool frame. Next, define  $p_{i-1,i}$  to be the constant  $\mathbb{R}^3$  vector from  $\mathcal{O}_{i-1}$  to  $\mathcal{O}_i$  represented in the  $i - 1$  frame, define  $p_{6T}$  to be the constant  $\mathbb{R}^3$  vector from  $\mathcal{O}_6$  to  $\mathcal{O}_T$  in the 6 frame, and define  $R_{6T}$  to be the constant orientation of the tool frame with respect to the 6 frame. Also define  $h_i$  to be the constant unit vector rotation axis for the  $i$ th joint represented in the  $i$  frame. Then, the rotation and position of the tool frame with respect to the world frame is

$$\begin{aligned} R_{0T} &= R_{01} R_{12} R_{23} R_{34} R_{45} R_{56} R_{6T}, \\ p_{0T} &= p_{01} + R_{01}(p_{12} + R_{12}(p_{23} + R_{23}(p_{34} \\ &\quad + R_{34}(p_{45} + R_{45}(p_{56} + R_{56} p_{6T}))))), \end{aligned} \quad (74)$$

where  $R_{i-1,i} = R(h_i, q_i)$  and  $q_i$  is the  $i$ th joint angle. We also use the convention that  $R_{i,i-1} = R(h_i, -q_i)$  and for  $j > i$ ,  $R_{ij} = R_{i,i+1} \cdots R_{j-1,j}$ .

The inverse kinematics problem for a robot with kinematic parameters  $\{p_{i-1,i}\}_{i=1}^6$ ,  $p_{6T}$ ,  $\{h_i\}_{i=0}^6$ ,  $R_{6T}$  means finding all joint angles  $q = [q_1 \ q_2 \ \cdots \ q_6]^T$  corresponding to a given end effector rotation and position  $(R_{0T}, p_{0T})$ . In general, one  $(R_{0T}, p_{0T})$  corresponds to multiple  $q$ , which are called the different inverse kinematics branches.

Rewriting (74) by moving constants to the left-hand side results in

$$\begin{aligned} R_{06} &= R_{0T} R_{6T}^T = R_{01} R_{12} R_{23} R_{34} R_{45} R_{56}, \\ p_{16} &= p_{0T} - R_{06} p_{6T} - p_{01} \\ &= R_{01}(p_{12} + R_{12}(p_{23} + R_{23}(p_{34} \\ &\quad + R_{34}(p_{45} + R_{45} p_{56}))))). \end{aligned} \quad (75)$$

This means the inverse kinematics procedures can be in terms of  $(R_{06}, p_{16})$ .

In the following inverse kinematics solutions, the problem is broken down into subproblems, and the solution for  $q$  branches each time a subproblem has multiple solutions. This means the procedures find all inverse kinematics solutions.

If a subproblem does not have any exact solution, then that inverse kinematics branch fails to have an exact solution. To keep track of which branches have valid solutions, one can keep track of which subproblems yielded exact solutions, or one can check that the forward kinematics matches the desired pose. In case only one inverse kinematics solution is required, only one branch can be chosen each time a subproblem has multiple solutions, either by picking  $q_i$  closest to the previous solution, or by picking  $q_i$  to be in a desired interval.

When a subproblem solution does not depend on  $\theta$ , such as when certain rotation axes are collinear, then the robot has a singularity for that inverse kinematics branch. The inverse kinematics procedure can return with a failure for that branch, or the joint angles from the previous solutions can be used for any arbitrary angles. It should be noted that using these inverse kinematics procedures for singular poses is not recommended as the internal robot motion is not parameterized and moving close to a singular direction will result in large joint motion.

The following solutions are valid not just for a single robot, but for a family of robots with certain conditions on their kinematics parameters based on consecutive intersecting or parallel joints. Therefore, a single code implementation can perform inverse kinematics for multiple robots in the same kinematic family but with different dimensions.

If a robot has three consecutive intersecting or parallel joint axes, then the inverse kinematics can be solved using Subproblems 5 or 6, respectively. If a robot has three intersecting or parallel joint axes and some other pair of intersecting or parallel axes, then the solution can sometimes be written in terms of just Subproblems 1, 2, 3, or 4. This is in accordance with the special simplified cases of Subproblems 5 and 6. If just one pair of consecutive joints are intersecting or parallel, then the problem can be reduced to a 1D search over a circle, again using Subproblems 5 or 6, respectively. If multiple pairs of consecutive joints are parallel or intersecting, then sometimes a 1D search may be performed using only Subproblems 1, 2, 3, or 4. In the fully general case where no consecutive joints are parallel or intersecting, then the problem reduces to a 2D search over a torus using Subproblem 5.

#### A. 6R Robots with Spherical Wrists

1) *General Solution:* Many industrial robots have spherical wrists, meaning  $(h_4, h_5, h_6)$  intersect at a point, as depicted in Fig. 8. (The solution is similar if the spherical joint is in the middle of the kinematic chain.) Choose the origins of frames 4, 5, 6 at the intersection so that  $p_{45} = p_{56} = 0$ . This allows us to decouple the position and rotation. For position,

$$p_{16} = R_{01}(p_{12} + R_{12}(p_{23} + R_{23}p_{34})), \quad (76)$$

which only depends on  $(q_1, q_2, q_3)$  and can be rearranged as

$$-R_{10}p_{16} + p_{12} + R_{12}(p_{23} + R_{23}p_{34}) = 0. \quad (77)$$

This is just Subproblem 5.

To solve for the wrist angles  $(q_4, q_5, q_6)$ , write the orientation equation as

$$R_{32}R_{21}R_{10}R_{06} = R_{34}R_{45}R_{56} \quad (78)$$

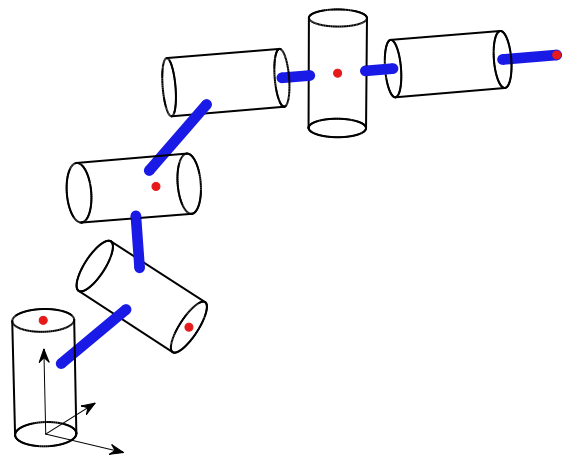


Fig. 8. 6R robot arm with a spherical joint at the robot wrist, meaning  $\mathcal{O}_4 = \mathcal{O}_5 = \mathcal{O}_6$ . Due to decoupling between position and rotation, the inverse kinematics can be solved using Subproblem 5 for the first three joints, and Subproblems 1 and 4 (or 1 and 2) for the last three joints.

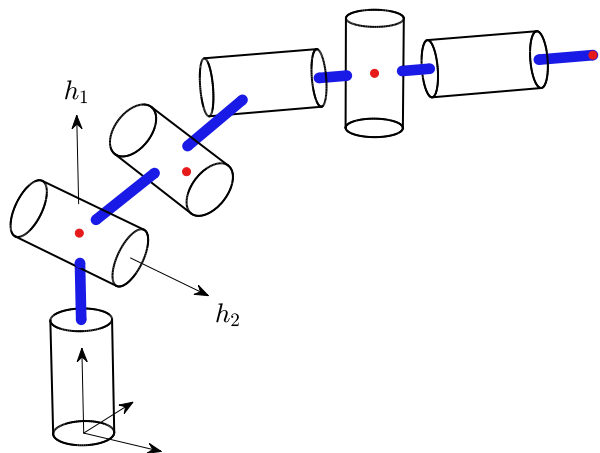


Fig. 9. 6R robot arm with a spherical wrist and the first two joint axes intersecting, meaning  $\mathcal{O}_1 = \mathcal{O}_2$ . The inverse kinematics of the first three joints can be solved using Subproblems 2 and 3.

For each  $(q_1, q_2, q_3)$ , the left-hand side is known, which can be called  $R_{36}$ . Project it to  $h_4$  and  $h_6$ :

$$h_4^T R_{36} h_6 = h_4^T R_{45} h_6, \quad (79)$$

and solve for two solutions of  $q_5$  using Subproblem 4. Then, find  $q_4$  by using Subproblem 1 to solve

$$R_{36} h_6 = R_{34} R_{45} h_6. \quad (80)$$

The joint angle  $q_6$  may be found in a similar way using Subproblem 1.

Alternatively, we can directly use (80) to solve for up to two solutions of  $(q_4, q_5)$  using Subproblem 2, and then solve for  $q_6$  using Subproblem 1.

2) *Two Intersecting Joint Axes:* Many industrial robots have the first two axes intersecting in addition to a spherical wrist, as depicted in Fig. 9. In this case,  $p_{12} = 0$ . Taking the norm of both sides of (76), we have

$$\|p_{16}\| = \|p_{23} + R_{23}p_{34}\|, \quad (81)$$

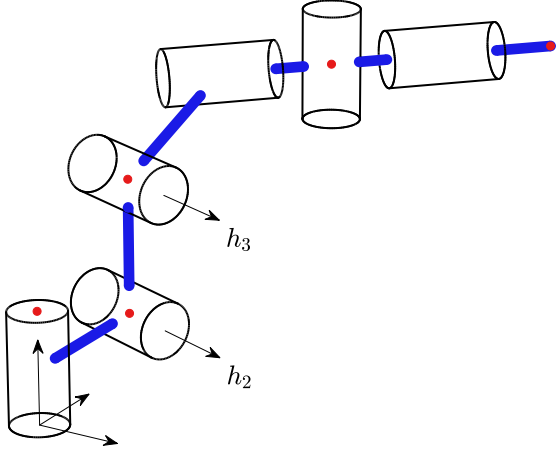


Fig. 10. 6R robot arm with a spherical wrist and two consecutive parallel joint axes  $h_2 = h_3$ . The inverse kinematics of the first three joints can be solved using Subproblems 1, 3 and 4.

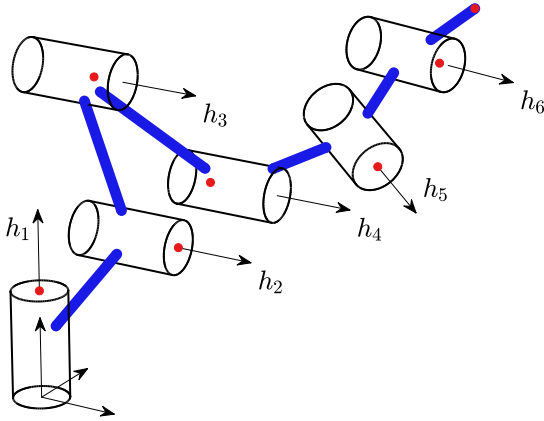


Fig. 11. 6R robot arm with three consecutive parallel axes  $h_2 = h_3 = h_4$ . Inverse kinematics can be solved using Subproblems 1, 3, and 6. If axes 5 and 6 intersect, then inverse kinematics can be solved using Subproblems 1, 3, and 4.

which may be solved using Subproblem 3 for up to two solutions of  $q_3$ . For each  $q_3$ , we can use Subproblem 2 to find up to two solutions of  $(q_1, q_2)$ , for a total of four solutions of  $(q_1, q_2, q_3)$ .

3) *Two Parallel Joint Axes*: Many industrial robots do not have  $p_{12} = 0$  but have parallel second and third joint axes (i.e.,  $h_2 = h_3$ ), in addition to a spherical wrist, as depicted in Fig. 10. Rearranging (77) and projecting onto  $h_2$ , we have

$$h_2^T R_{10} p_{16} = h_2^T (p_{12} + p_{23} + p_{34}), \quad (82)$$

which may be solved using Subproblem 4 for up to two solutions of  $q_1$ . For each  $q_1$ , we can use Subproblem 3 to find up to two solutions of  $q_3$ . For each of the four possible  $(q_1, q_3)$ , we can solve for the corresponding  $q_2$  using Subproblem 1.

### B. 6R Robots with Three Parallel Axes

Some robots have three consecutive parallel joint axes, say  $h_2 = h_3 = h_4$ , as depicted in Fig. 10. In this case,

$$h_2^T (R_{12} p_{23} + R_{13} p_{34} + R_{14} p_{45}) = h_2^T (p_{23} + p_{34} + p_{45}). \quad (83)$$

Write the position portion of (75) as

$$p_{16} = R_{01} p_{12} + R_{01} R_{14} R_{45} p_{56} + R_{01} (R_{12} p_{23} + R_{13} p_{34} + R_{14} p_{45}). \quad (84)$$

Projecting onto  $h_2$ , we have

$$h_2^T R_{10} p_{16} - h_2^T R_{45} p_{56} = h_2^T (p_{12} + p_{23} + p_{34} + p_{45}). \quad (85)$$

From the orientation portion of (75), we have

$$h_2^T R_{10} R_{06} h_6 = h_2^T R_{45} h_6 \quad (86)$$

If  $p_{56}$  is the zero vector, we can find up to two solutions of  $q_1$  from (85) using Subproblem 4. For each solution of  $q_1$ , we can use Subproblem 4 to solve for up to two solutions of  $q_5$  from (86) for a total of four solutions. If  $p_{56} \neq 0$ , (85) and (86) form a system of equations which can be solved using Subproblem 6 for up to four solutions of  $(q_1, q_5)$ .

From the orientation portion of (75), we can solve for  $q_2 + q_3 + q_4$  (and hence  $R_{14}$ ) using Subproblem 1. We can solve for up to two solutions of  $q_3$  using Subproblem 3 for a total of eight solutions. Within these eight solutions, we can solve for  $q_2$  using Subproblem 1, solve for  $q_4$  using subtraction (wrapping the result to  $[-\pi, \pi]$  if desired), and  $q_6$  using Subproblem 1.

### C. General 6R Robot Inverse Kinematics

1) *General Case: 2D Search*: A general 6R robot does not have a closed-form inverse kinematics solution. Therefore, some type of search is needed. A common method is to use gradient descent using the arm Jacobian for the descent direction starting with an initial guess. Such a method can only find one inverse kinematic solution for each initial guess, can be computationally inefficient, and can have a configuration-dependent computation time for the same convergence criterion. We propose a search-based method over the surface of a torus which can find all solutions through exhaustive search on a two-dimensional grid, though for the same level of accuracy the computation time would still be configuration dependent.

Given  $(q_1, q_2)$ , we have  $R_{01}$  and  $R_{12}$ . We can then solve for up to four solutions of  $(q_3, q_4, q_5)$  using Subproblem 5:

$$-p_{34} + R_{32} (R_{21} (R_{10} p_{16} - p_{12}) - p_{23}) = R_{34} (p_{45} + R_{45} p_{56}). \quad (87)$$

With each  $(q_1, q_2, q_3, q_4, q_5)$ , compute either of the error measures

$$e_1 = \|R_{01} R_{12} R_{23} R_{34} R_{45} h_6 - R_{06} h_6\|, \quad (88a)$$

$$e_2 = |(R_{01} R_{12} R_{23} R_{34} R_{45} h_6)^T R_{06} h_6 - 1|. \quad (88b)$$

Search through  $(q_1, q_2)$  within the joint limits to find the zeros of  $e$ . For each zero of  $e$ , solve for  $q_6$  using Subproblem 1:

$$R_{56} p = (R_{01} R_{12} R_{23} R_{34} R_{45})^T R_{06} p \quad (89)$$

where  $p$  is any vector not collinear with  $h_6$ .

2) *Two Intersecting Axes: 1D Search:* If  $p_{56} = 0$ , then (87) becomes

$$-p_{12} + R_{10}p_{16} = R_{12}(p_{23} + R_{23}(p_{34} + R_{34}p_{45})) \quad (90)$$

In this case, for each  $q_4$ , we can find up to four solutions of  $(q_1, q_2, q_3)$  using Subproblem 5. For each of these solutions, we can find up to two solutions of  $(q_5, q_6)$  by using Subproblem 2 to solve

$$(R_{01}R_{12}R_{23}R_{34})^T R_{06}h_5 = R_{45}R_{56}h_5. \quad (91)$$

Finally, perform a line search on  $q_4$  to find all the zeros of (88). A similar procedure may be applied if  $p_{23} = 0$  and  $p_{56} \neq 0$ .

#### D. Least-Squares Inverse Kinematics

Since Subproblems 1, 2, 3 and 4 are posed as minimizations, inverse kinematics procedures using these subproblems can yield solutions even if the exact solution does not exist. The resulting pose of the robot end effector with these solutions may be close to the desired pose, which is helpful for a number of reasons. Even if the desired pose is feasible, in case of any intermediate numerical inaccuracies in the inverse kinematics procedure, the least-squares solutions for each subproblem means that the final result of  $q$  stays accurate. If the desired pose is nearly outside the workspace (say, because the desired pose is on the workspace boundary and numerical issues have caused the pose to move outside the workspace), then the inverse kinematics procedure will still give a close solution.

If the desired pose is far from the feasible workspace, then the resulting pose is still close in some sense, but in general it is unclear in what sense it is close. For certain robot configurations, we can be precise and say that the resulting pose solves the constrained least-squares minimization

$$\min_q \|p_{0T}(q) - p_{0T}^{des}\| \quad \text{s.t. } R_{0T}(q) = R_{0T}^{des}, \quad (92)$$

where  $(R_{0T}^{des}, p_{0T}^{des})$  is the desired end effector rotation and position. This means that the rotation is exactly as desired, and the position is as close as possible in the usual Euclidean sense.

One robot configuration that achieves (92) is a 6R robot with a spherical wrist, two parallel axes, and a few other constraints. In addition to the constraints  $p_{45} = p_{56} = 0$  and  $h_2 = h_3$ , we must have  $h_2^T(p_{12} + p_{23} + p_{34}) = 0$ ,  $h_1^T h_2 = 0$ , and  $p_{6T} = 0$ . We also need  $h_4^T h_5 = 0$  and  $h_5^T h_6 = 0$  so the spherical wrist can achieve any orientation. Under these conditions, we are minimizing distances in a cylindrical coordinate system.

If in addition to the above  $p_{12} = 0$ , then (92) is also achieved with the algorithm for robots with spherical wrists and two intersecting axes. Or, if in addition to the above  $h_2 = h_3 = h_4$ , then (92) is achieved using the algorithm for robots with three parallel axes and two intersecting axes.

## V. EVALUATION

The subproblem solutions and inverse kinematics solutions were implemented in MATLAB, and the computation times to run these solutions were measured. The seven subproblem solutions were programmed to return any exact or least-squares

TABLE II  
SUBPROBLEM SOLUTION RUNTIMES

Subproblem	m-file ( $\mu\text{s}$ )	MEX ( $\mu\text{s}$ )
1: Cone and point	$5 \pm 0.29$	$19 \pm 1.20$
2: Two cones	$22 \pm 0.81$	$25 \pm 0.72$
2E: Two offset cones	$24 \pm 0.53$	$23 \pm 0.87$
3: Cone and sphere	$9 \pm 0.36$	$20 \pm 0.26$
4: Cone and plane	$7 \pm 0.59$	$20 \pm 0.70$
5: Three cones	$95 \pm 3.89$	$41 \pm 0.42$
6: Four cones	$114 \pm 1.88$	$45 \pm 1.17$

solutions, and when applicable also return a flag to indicate if the solution is least squares. The five robot inverse kinematics solutions which do not involve searching were programmed to return all solutions, and to provide least-squares solutions when possible, along with a flag to indicate if the solution is least squares. The two inverse kinematics solutions that involve a 1D or 2D search were implemented by sampling the search space with an evenly spaced grid, and then performing a derivative-free optimization using the sample with the smallest error as the initial guess, which returns one inverse kinematics solution.

The timing was also measured after compiling the MATLAB m-file code into a C++ MEX file using MATLAB coder, which can often speed up computation. This file is called from MATLAB, and therefore has overhead compared to running a similar C++ function from other C++ code. Furthermore, for the inverse kinematics solutions, timing was measured after compiling into MEX and also hardcoding the robot kinematics parameters into the function, using one robot for each inverse kinematics algorithm. The robot examples include real 6-dof robots, as well as 7-dof robots with one fixed joint angle. Two robot kinematics parameters were made up (Spherical-Bot and Three-Parallel-Bot).

To test each subproblem implementation, 100 trials were performed with a random set of input parameters which yielded at least one exact solution. The means and standard deviations for the subproblem timing results are shown in Table II.

To test each robot inverse kinematics implementation, 100 trials were performed (with some exceptions) using randomly chosen kinematics parameters (except in the hardcoded kinematics cases) and a randomly chosen achievable pose. For some of the two inverse kinematics cases involving a 1D or 2D search, ten trials were performed instead of 100. The means and standard deviations for the inverse kinematics timing results are shown in Table III.

Timing trials were performed in MATLAB R2022b according to the MATLAB timing measurement whitepaper [34]. The timing for one function was measured by running the function enough times so that the total execution time was between 0.01 and 0.001 seconds, (or at least ten times for longer-running functions), and then dividing the total execution time by the number of times run. The measurement was performed on a computer with an Intel Core i7-3770K CPU at 3.50 GHz and 16 GB memory running Windows 10. The computer was recently restarted, had networking disabled, had antivirus disabled and many other programs terminated, and had MATLAB

TABLE III  
ROBOT INVERSE KINEMATIC SOLUTION RUNTIMES

Robot Type	m-file ( $\mu\text{s}$ )	MEX ( $\mu\text{s}$ )	Hardcoded MEX ( $\mu\text{s}$ )	Hardcoded Robot
General 6R (2D search)	$359695 \pm 5738.60$	$19751 \pm 181.61$	$19672 \pm 121.40$	ABB YUMI [29], fixed $q_3$
Two intersecting axes (1D search)	$31786 \pm 508.66$	$895 \pm 14.34$	$460 \pm 6.76$	RRC K-1207i [30], fixed $q_6$
Spherical wrist	$707 \pm 19.19$	$49 \pm 1.74$	$44 \pm 1.25$	Spherical-Bot
and two intersecting axes	$627 \pm 20.05$	$39 \pm 1.22$	$34 \pm 0.88$	KUKA LBR iiwa 7 R800 [31], fixed $q_3$
and two parallel axes	$608 \pm 9.07$	$38 \pm 1.03$	$34 \pm 0.58$	ABB IRB 6640 [32]
Three parallel axes	$442 \pm 22.74$	$53 \pm 1.40$	$51 \pm 1.19$	Three-Parallel-Bot
and two intersecting axes	$272 \pm 15.78$	$37 \pm 1.06$	$33 \pm 0.73$	UR5 [33]

set to realtime priority.

The subproblem timing results show that all subproblems can be solved in under  $50 \mu\text{s}$  after compiling to MEX. Subproblems 1, 2, 3, and 4 run so quickly that compiling to MEX actually increases executing time due to the MEX overhead.

The robot inverse kinematics timing results show that all closed-form solutions can run in under  $55 \mu\text{s}$  after compiling to MEX. The fastest algorithm ran in  $33 \mu\text{s}$ , which is a frequency of over 30 kHz. 1D and 2D searches show a significant increase in execution time due to sampling the search space. Despite this, even the general 6-dof robot, which requires a 2D search, can run at over 50 Hz.

There are a number of ways to speed up computation time for the subproblem solutions and inverse kinematics solutions. One easy way to speed up computation is to implement the algorithms on a faster computer and in a lower-level language like C++, which avoids the overhead of m-files or MEX. Although some work was put into optimizing the implementations for Subproblems 1-4, there is likely still room for improvement in the implementations of Subproblems 5 and 6. The inverse kinematics solutions are not optimized; for example, nearly half of the computation time for most of the inverse kinematics algorithms is spent computing rotation matrices. For the closed-form inverse kinematics solutions, the algorithm can be sped up if only one pose is required, as currently they output all solutions. For the search-based inverse kinematics algorithms, sampling could be parallelized, and a much faster search method could be used, such as one that immediately starts optimization after just a few random samples, doing a random restart if that optimization fails. The search-based algorithms would also be much faster if they had a close previous pose as an initial guess; in that case, no sampling would be required, and the optimization would terminate after only a few iterations.

## VI. CONCLUSION

This paper revisits the subproblem decomposition method for solving robot inverse kinematics. We added three more subproblems to the original three Paden–Kahan subproblems along with one subproblem extension (together Subproblems 1-6) all with closed-form solutions, and for Subproblems 1, 2, 3, and 4, we found the least-squares solutions in closed form when the exact problem has no solution. Subproblems 4 and 6 have not appeared in the literature in the past. Our approach converts a nonlinear subproblem to a linear

one and then imposes constraints on the linear solutions. It is easy to understand and visualize and is computationally efficient. Implementation code in MATLAB is provided and is computationally efficient, and even further code optimization is possible to gain additional computational performance. The inverse kinematics for many common types of robots may be decomposed into a series of subproblems and solved directly in closed form. Furthermore, when the solution does not exist, our method finds the least-squares solution without iteration. For a general 6R robot, the decomposition method reduces the solution to a 1D search on a circle or 2D search on a torus. This method finds *all* inverse kinematics solution instead of just one solution close to the initial guess as in the Jacobian-based methods. There may be applications for these subproblems beyond just inverse kinematics for 6R arms. For example, we can use these subproblems to solve inverse kinematics for 7-DOF arms if some parameterization for the redundant degree of freedom is also given. These subproblems may also be useful in computer graphics and animation.

While these subproblem solutions help find closed-form solutions to many robots, there are still certain robots with closed-form solutions which cannot be solved using these subproblems. For example, a 2R-2R-2R robot with perpendicular axes at each 2R joint does have a closed-form solution but cannot be solved with these subproblems at this point. Although our solutions are in closed form as they only involve solving polynomials up to a quartic, in practice there is little issue with solving higher-order polynomials efficiently. This means it would be useful to solve other subproblems by reducing them to these higher-order polynomials, as is done in [1]. Doing this would allow us to avoid having to do a 1D or 2D search for the general robot cases.

## REFERENCES

- [1] D. L. Pieper, *The kinematics of manipulators under computer control*. Stanford University, 1969.
- [2] B. E. Paden, "Kinematics and control of robot manipulators," Ph.D. dissertation, EECS Department, University of California, Berkeley, Jan 1986. [Online]. Available: <http://www2.eecs.berkeley.edu/Pubs/TechRpts/1986/631.html>
- [3] R. Murray, Z. Li, and S. Sastry, *A Mathematical Introduction to Robotic Manipulation*. Boca Raton, FL: CRC Press, 1994.
- [4] I. Dimovski, M. Trompeska, S. Samak, V. Dukovski, and D. Cvetkoska, "Algorithmic approach to geometric solution of generalized Paden–Kahan subproblem and its extension," *International Journal of Advanced Robotic Systems*, vol. 15, no. 1, 2018.
- [5] T. Yue-sheng and X. Ai-ping, "Extension of the second Paden–Kahan sub-problem and its' application in the inverse kinematics of a manipulator," in *2008 IEEE Conference on Robotics, Automation and Mechatronics*, 2008, pp. 379–381.

- [6] Q. Chen, S. Zhu, and X. Zhang, "Improved inverse kinematics algorithm using screw theory for a six-DOF robot manipulator," *International Journal of Advanced Robotic Systems*, vol. 12, no. 10, p. 140, 2015.
- [7] H. S. An, T. W. Seo, and J. W. Lee, "Generalized solution for a sub-problem of inverse kinematics based on product of exponential formula," *Journal of Mechanical Science and Technology*, vol. 32, no. 5, pp. 2299–2307, 2018.
- [8] H. Wang, X. Lu, Z. Zhang, Y. Li, C. Sheng, and L. Gao, "A novel second subproblem for two arbitrary axes of robots," *International Journal of Advanced Robotic Systems*, vol. 15, no. 2, 2018.
- [9] H. Wang, X. Lu, C. Sheng, Z. Zhang, W. Cui, and Y. Li, "General frame for arbitrary 3R subproblems based on the POE model," *Robotics and Autonomous Systems*, vol. 105, pp. 138–145, 2018.
- [10] M. Kong, Z. Du, L. Sun, and Y. Zhang, "Solution and application of two inverse kinematics subproblems," in *2006 International Conference on Mechatronics and Automation*. IEEE, 2006, pp. 1164–1168.
- [11] J. Xu, Z. Liu, Q. Cheng, Y. Zhao, Y. Pei, and C. Yang, "Models for three new screw-based IK sub-problems using geometric descriptions and their applications," *Applied Mathematical Modelling*, vol. 67, pp. 399–412, 2019.
- [12] I.-M. Chen and Y. Gao, "Closed-form inverse kinematics solver for reconfigurable robots," in *Proceedings 2001 ICRA. IEEE International Conference on Robotics and Automation (Cat. No. 01CH37164)*, vol. 3. IEEE, 2001, pp. 2395–2400.
- [13] J. Leoro, T. Hsiao, and C. Betancourt, "A new geometric subproblem to extend solvability of inverse kinematics based on screw theory for 6R robot manipulators," *International Journal of Control, Automation and Systems*, vol. 19, no. 1, pp. 562–573, 2021.
- [14] J. Zhao, W. Wang, Y. Gao, and H. Cai, "Generation of closed-form inverse kinematics for reconfigurable robots," *Frontiers of Mechanical Engineering in China*, vol. 3, no. 1, pp. 91–96, 2008.
- [15] H. Wang, X. Lu, W. Cui, Z. Zhang, Y. Li, and C. Sheng, "General inverse solution of six-degrees-of-freedom serial robots based on the product of exponentials model," *Assembly Automation*, 2018.
- [16] E. Sariyildiz and H. Temeltas, "A comparison study of three screw theory based kinematic solution methods for the industrial robot manipulators," in *2011 IEEE International Conference on Mechatronics and Automation*. IEEE, 2011, pp. 52–57.
- [17] Y. S. Tan, P. L. Cheng, and A. P. Xiao, "Solution for a new sub-problem in screw theory and its' application in the inverse kinematics of a manipulator," in *Applied Mechanics and Materials*, vol. 34. Trans Tech Publ, 2010, pp. 271–275.
- [18] —, "Inverse kinematics solution for a 6R special configuration manipulators based on screw theory," in *Advanced Materials Research*, vol. 216. Trans Tech Publ, 2011, pp. 250–253.
- [19] J. M. Pardos-Gotor, *Screw Theory in Robotics: An Illustrated and Practicable Introduction to Modern Mechanics*. CRC Press, 2021.
- [20] T. Song, B. Pan, G. Niu, J. Yan, and Y. Fu, "General closed-form inverse kinematics for arbitrary three-joint subproblems based on the product of exponential model," *Frontiers of Mechanical Engineering*, vol. 17, no. 2, pp. 1–17, 2022.
- [21] P.-F. Lin, M.-B. Huang, and H.-P. Huang, "Analytical solution for inverse kinematics using dual quaternions," *IEEE Access*, vol. 7, pp. 166 190–166 202, 2019.
- [22] L. Chen, T. Zielinska, J. Wang, and W. Ge, "Solution of an inverse kinematics problem using dual quaternions," *International Journal of Applied Mathematics and Computer Science*, vol. 30, no. 2, 2020.
- [23] L. Josuet, B. Carlos, L. Hsien, H. Te-Sheng, W. Chun-Sheng *et al.*, "An improved inverse kinematics solution of 6R-DOF robot manipulators with euclidean wrist using dual quaternions," in *2016 International Automatic Control Conference (CAC)*. IEEE, 2016, pp. 77–82.
- [24] M. D. Shuster and F. L. Markley, "Generalization of the Euler angles," *The Journal of the Astronautical Sciences*, vol. 51, no. 2, pp. 123–132, 2003.
- [25] A. Norrdine, "An algebraic solution to the multilateration problem," in *Proceedings of the 15th International Conference on Indoor Positioning and Indoor Navigation, Sydney, Australia*, vol. 1315, 2012.
- [26] W. Shanda, L. Xiao, L. Qingsheng, and H. Baoling, "Existence conditions and general solutions of closed-form inverse kinematics for revolute serial robots," *Applied Sciences*, vol. 9, no. 20, p. 4365, 2019.
- [27] L. Euler, "Nova methodus motum corporum rigidorum degerminandi," *Novi commentarii academiae scientiarum Petropolitanae*, pp. 208–238, 1776.
- [28] O. Rodrigues, "Des lois géométriques qui régissent les déplacements d'un système solide dans l'espace, et de la variation des coordonnées provenant de ces déplacements considérés indépendamment des causes qui peuvent les produire," *J. Math. Pures Appl*, vol. 5, no. 380–400, p. 5, 1840.
- [29] ABB, "IRB 14000 YuMi - collaborative robot," <https://new.abb.com/products/robotics/collaborative-robots/yumi/irb-14000-yumi>, 2022, (accessed Oct. 31, 2022).
- [30] Robotics Research Corporation, "Dexterous manipulators and advanced control systems," Robotics Research Corporation, Tech. Rep., 2005, Accessed Oct. 31, 2022. [Online]. Available: [http://www.robotics-research.com/RRC\\_TechDoc.PDF](http://www.robotics-research.com/RRC_TechDoc.PDF)
- [31] KUKA, "LBR iiwa," <https://www.kuka.com/en-us/products/robotics-systems/industrial-robots/lbr-iiwa>, 2022, (accessed Oct. 31, 2022).
- [32] ABB, "IRB 6640," <https://new.abb.com/products/3HAC020536-012/irb-6640>, 2022, (accessed Oct. 31, 2022).
- [33] Universal Robots, "UR5 collaborative robot arm," <https://www.universal-robots.com/products/ur5-robot/>, 2022, (accessed Oct. 31, 2022).
- [34] B. McKeeman, "Measuring MATLAB performance," MathWorks, Tech. Rep., August 2008. [Online]. Available: <https://www.mathworks.com/matlabcentral/fileexchange/18510-matlab-performance-measurement>